Evaluation of Collision Cross Section Calibrants for Structural Analysis of Lipids by Traveling Wave Ion Mobility-Mass Spectrometry

Kelly M. Hines,[†] Jody C. May,[‡] John A. McLean,[‡] and Libin Xu*,[†]

[†]Department of Medicinal Chemistry, University of Washington, Seattle, Washington 98195, United States
[‡]Department of Chemistry, Center for Innovative Technology, Vanderbilt Institute of Chemical Biology, Vanderbilt Institute for Integrative Biosystems Research and Education, Vanderbilt University, Nashville, Tennessee 37235, United States

S *Supporting Information*

ABSTRACT: Collision cross section (CCS) measurement of lipids using traveling wave ion mobility-mass spectrometry (TWIM-MS) is of high interest to the lipidomics field. However, currently available calibrants for CCS measurement using TWIM are predominantly peptides that display quite different physical properties and gas-phase conformations from lipids, which could lead to large CCS calibration errors for lipids. Here we report the direct CCS measurement of a series of phosphatidylcholines (PCs) and phosphatidylethanolamines (PEs) in nitrogen using a drift tube ion mobility (DTIM) instrument and an evaluation of the accuracy and reproducibility of PCs and PEs as CCS calibrants for phospholipids against different classes of calibrants, including polyalanine (PolyAla), tetraalkylammonium salts (TAA), and hexakis(fluoroalkoxy)phosphazines (HFAP), in both positive and negative modes in TWIM-MS analysis. We demonstrate that structurally mismatched calibrants lead to larger errors in calibrated CCS values while the structurally matched calibrants, PCs and PEs, gave highly accurate and reproducible CCS values at different traveling wave parameters. Using the lipid calibrants, the majority of the CCS values of several classes of phospholipids measured by TWIM are within 2% error of the CCS values measured by DTIM. The development of phospholipid CCS calibrants will enable high-accuracy structural studies of lipids and add an additional level of validation in the assignment of identifications in untargeted lipidomics experiments.
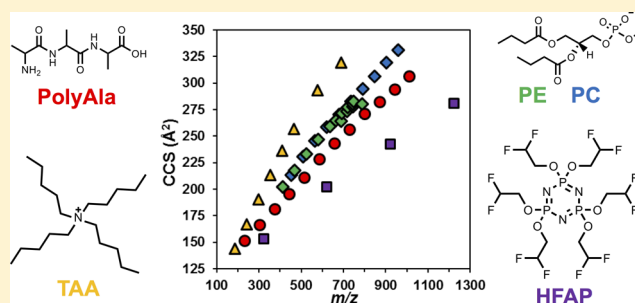
L ipids are essential components of cell membranes and play important roles in normal physiology[1,2] as well as in human diseases such as atherosclerosis,[3] cancer,[4,5] and diabetes.[6] Over the past decade, the study of the complete profile and pathways of lipids in biological systems, or lipidomics, has emerged as an important new area of "omics" studies,[7−10] making up a major component of metabolomics that is complementary to genomics, transcriptomics, and proteomics. Advances in lipidomics strategies are largely driven by the advancement of the mass spectrometry (MS) techniques, which have led to two commonly used methodologies: shotgun lipidomics[11,12] and liquid chromatography (LC)−MS-based lipidomics.[8,13,14] However, one major challenge for lipidomics studies remains: the narrow mass-to-charge (m/z) window (m/z 600−900) in which lipids are observed leads to a large number of lipid ions having the same (i.e., isobaric) mass, which obscures the definitive identification of many lipids. This challenge can be addressed by ion mobility-mass spectrometry (IM-MS),[15−19] which provides an orthogonal dimension of separation on the basis of gas-phase structure and aids in the unambiguous identification of isobaric lipid species.[20−25]

The separation of ions in the low-field IM experiment is based on differences in the ion-neutral collision cross section

(CCS) as the ions drift through a neutral background gas, commonly helium or nitrogen, under the influence of a static electric field (as in drift tube IM, DTIM)[21,26,27] or a dynamic electric field (as in traveling wave IM, TWIM).[28,29] When coupled with MS, a two-dimensional separation is achieved, which provides important molecular information due to the relationship between mass (as indicated by the mass-to-charge, m/z) and CCS (as indicated by t_d) in the form of structural density.[15−18] As a result, different classes of biological molecules can be separated by IM-MS based on differences in their gas phase packing efficiencies, where densely packed biomolecules occur with a smaller CCS (shorter t_d) than loosely packed species of a similar mass. As such, each class of biomolecule occupies a discrete region of IM-MS space with lipids on average occupying the largest CCSs, followed by peptides, carbohydrates, and oligonucleotides.[21−23] Structural separations may also be observed within a biomolecular class, such as the separation of sphingolipids and glycerophospholipids subspecies within the lipid class.[21,24,26,30,31]

Because of the wide availability of commercial TWIM instruments, CCS measurement on the TWIM platform is of high interest. While CCS values can be directly determined from DTIM analysis using the Mason−Schamp equation,[32,33] a precise relationship between CCS and t_d in TWIM has not yet been developed, although some progress has been made toward understanding the theory of TWIM.[34−36] Thus, in order to determine CCS values using TWIM, it is necessary to determine a calibration relationship between ions with known CCS values obtained on DTIM instrumentation and the t_d measured in TWIMS. Commonly, a power regression analysis is used for calibrating TWIM data to CCS as it has been observed that CCS and t_d follow an empirical power function relationship in TWIM,[30,37−42] although both linear[39,43] and binomial regressions have also been utilized for TWIM calibration purposes.[41]

Major efforts have been devoted to developing TWIM calibration strategies for the analysis of peptides and proteins, such as the use of tryptic peptides,[30,39] denatured or native proteins,[37,38,40,44] and polyalanines (PolyAla).[41] Small-molecule calibrants for masses of up to 609 Da have also been reported.[45] In recent years, PolyAla have become the most widely used calibrant series due to their long-term stability, even distribution of ions over a wide range of m/z and CCS, and ability to form several charge states.[41] Calibration of TWIM CCSs using PolyAla has been reported in the literature for use with a range of molecules, including small metabolites and lipids in both positive and negative modes.[24,42,46,47] However, it has been found on several occasions that TWIM calibration using ions that are of different physical properties could lead to large errors in calibrated CCSs. For example, calibration of lipids using tryptic peptides led to errors up to 6.4%.[30] In addition, Bush et al. found that for CCS measurements of native proteins, native protein calibrants alone performed better than a combination of native and denatured proteins or denatured proteins alone.[44] These errors are the result of commonly observed differences between molecular classes: (i) there is a mismatch in the m/z range in which the calibrants and the analytes occur as observed in Bush et al.[44] and (ii) the calibrant and analyte experience different forces in the TWIM separation, such as the ion−dipole interactions due to polarizability of the N_2 drift gas, which cause their drift times to scale differently with CCS.[48−50] To avoid errors in calibrated CCSs due to the above and other sources, calibration using ions with similar physical properties is desirable in order to achieve the highest CCS accuracy. Because of the large structural differences between the lipid ions and those of other classes of molecules in the gas phase,[21−23] designated lipid CCS calibrants are needed for TWIM analysis.

In this work, we report the direct CCS measurements of a series of phosphatidylcholines (PCs) and phosphatidylethanol-amines (PEs) (ranging from m/z 400 to 1000) in nitrogen using DTIM in both positive and negative-ion modes specifically for use as lipid CCS calibrants in other IM instrumentation. The PE and PC series were evaluated against different classes of calibrants, including PolyAla, tetraalkylam-monium salts (TAA), and hexakis(fluoroalkoxy)phosphazines (HFAP), in both positive and negative modes to determine their accuracy and reproducibility for calibration of lipid CCSs from TWIM analysis. We demonstrate that structurally mismatched calibrants lead to larger error in calibrated CCS values and establish two sets of structurally matched lipid calibrants, PCs and PEs, for generating highly accurate CCS

values of lipids in TWIM analysis. To our knowledge, this work represents the first systematic comparison of the effect of several structurally distinct classes of calibrants on TWIM CCS measurement, and the CCS of many of the lipid species presented here have not yet been measured by DTIM, particularly in the context of both positive and negative ion forms.

■ EXPERIMENTAL SECTION

Materials. A total of 10 phosphatidylcholine (PC) and 14 phosphatidylethanolamine (PE) lipid standards (Avanti Polar Lipids) with fatty acid tails ranging from 6 to 24 carbons were prepared as separate samples for analysis in positive and negative modes (see Table S1 for a list of lipid species and Avanti Polar Lipid catalog numbers). For positive mode analysis, mixtures of PCs and PEs were prepared at 5−10 μM (concentration of each species noted in Table S1) in methanol (Sigma-Aldrich) with 0.1% formic acid (Fisher Scientific). For negative mode analysis, mixtures of PEs and PCs were prepared at 5−10 μM (concentration of each species noted in Table S1) in methanol with 50 μM sodium hydroxide (Fisher Scientific) and 150 μM ammonium acetate (Fisher Scientific), respectively. Poly-DL-alanine (Sigma-Aldrich) was prepared at 25 μg/mL in 1:1 acetonitrile/water (Fisher Scientific) with 0.1% formic acid for positive mode analysis and without formic acid for negative mode analysis. A mixture of tetraalkylammonium bromide salts (TAA3, 5, 8 and 10, Acros Organics; TAA4, 6, 7, and 12, Sigma-Aldrich) was prepared at 1 ng/mL in methanol. A mixture of hexakis-(fluoroalkoxy)phosphazines (HFAP, ESI-L low concentration tuning mixture, Agilent Technologies, Santa Clara, CA) was prepared by 1:4 dilution with 95% acetonitrile in water. Sphingomyelin (SM, porcine brain), phosphatidyl serines (PS, porcine brain), PE (porcine brain), and PC (chicken egg) mixtures (Avanti Polar Lipids) were prepared as 10 μM solutions in 95% acetonitrile in water.

DTIM CCS Measurements. CCS measurements for PolyAla, PEs, PCs, and HFAP were performed in positive and negative ESI modes using an Agilent 6560 IM-MS with nitrogen drift gas as described previously.[26] The IM spectrometer portion of the instrument was operated under conditions which optimize the IM resolving power between 50 and 60 ($t/\Delta t$).[51] PE and PC lipids were detected as protonated and sodium coordinated adducts in the positive mode analysis, whereas $[M − H]^-$ and $[M + CH_3COO]^-$ species were observed in negative mode for PE and PC lipids, respectively. CCS values were determined from the Mason−Schamp equation as described previously.[26] For all ions, the CCS measurement precision was observed to be less than 1% RSD (see Tables S1−S3 for RSDs for each ion individually), and mass measurement accuracy was ≤5 ppm. Negative mode measurements were performed on 2 separate days, and the reported CCS values represent the weighted average of the two experiments ($n = 9$ per day).

TWIM Analysis and CCS Calibration. TWIM experiments were performed over 3 days, with three data acquisitions (positive mode, 1 min; negative mode, 2 min) per day for a total of nine data points. Samples were directly infused into the ESI source of a Waters Synapt G2-Si HDMS (Waters Corp., Milford, MA) at 10 μL/min for positive mode and 30 μL/min for negative mode. Data was acquired over m/z 50−1200 (to 1400 for HFAPs) in resolution mode ($m/\Delta m = 20\,000$) with 550 m/s TWIM wave velocity and 40 V wave height (see the
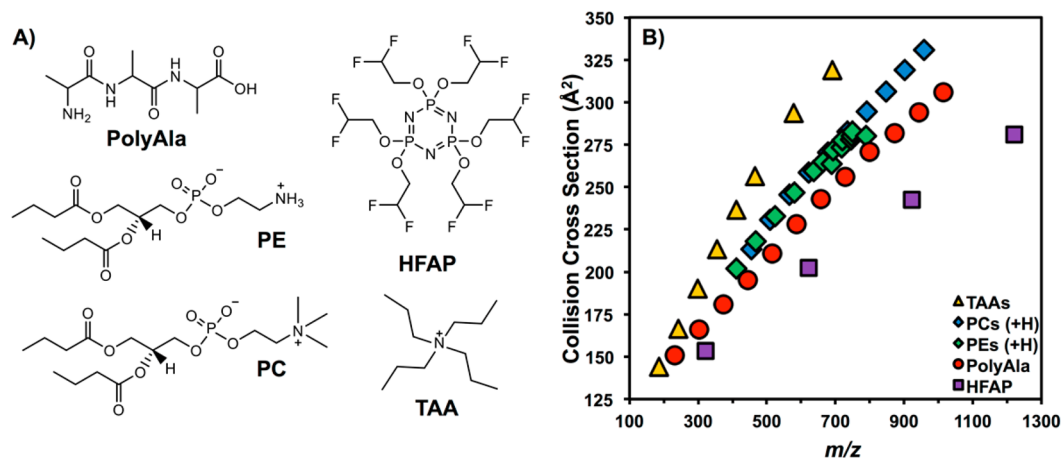
Figure 1. (A) Structures of select or exemplary species in each class of TWIM CCS calibrant (from left to right): polyalanine (PolyAla; trialanine shown); hexakis(fluoroalkoxy)phospazines (HFAP; hexakis(2,2-difluoroethoxy)phosphazine shown); phosphatidylethanolamine (PE; PE 4:0/4:0 shown); phosphatidylcholine (PC; PC 4:0/4:0 shown); tetralkylammonium salts (TAA; tetrapropylammonium shown). (B) IM-MS conformational space plot showing the trends in CCS-*m/z* for each of the five calibrants from + ESI DTIM-MS measurements in N$_2$. For clarity, only the protonated adducts of the PE and PC calibrants are shown.

Supporting Information for source and IM parameters). Additional experiments for validation were performed at varied wave heights and velocities (30, 35, 40 V and 450, 500, 550 m/s, respectively) and data was acquired over *m/z* 50−5000 to prevent roll over into the next IM cycle at lower wave heights. Additionally, data was acquired using a ramped wave velocity of 900−300 m/s (tuned to prevent roll over into the next IM cycle) and 40 V over *m/z* 50 to 1200 (to 1400 for HFAPs). For the analysis of lipid extracts, CCS calibration was performed against the PC sodium adducts using a 500 m/s wave velocity and 40 V wave height.

Drift times were obtained for each analyte by generating an extracted ion chromatogram (XIC) from the arrival time distribution function in MassLynx v4.1 using the monoisotopic mass and a mass window of ±0.075 Da. XICs were smoothed using the mean method (1 smooth; window size, ±1 scan) prior to reading the drift time from the peak apex. TWIM drift times (t_d, ms) and DTIM CCS (Ω, Å^2) values were corrected as described previously.[38] The calibration curves were generated in GraphPad Prism 5 by fitting the corrected drift time, $t_d{}'$, and the corrected CCS, Ω', to an equation of the form

$$\Omega' = zA'(t_d{}' - t_0)^B \qquad (1)$$

where A', t_0, and B are fit parameters and z is the ion charge state. This equation was used to account for ion flight time in areas outside the IM cell, t_0, and this method has been demonstrated to result in better correlation to the regression model and more accurate CCS values than the simple power regression model (without the t_0 term).[42]

In both positive and negative modes, the three intraday replicates were treated independently during the CCS calibration process (i.e., the number of points analyzed in negative mode for PEs and PCs were 42 and 30, respectively). Both species (+ H and + Na) observed in positive mode were similarly treated independently, such that the total number of points analyzed for PEs and PCs in positive mode were 85 and 60, respectively. Reported CCSs represent the average of nine experiments and interday RSDs were below 0.5% for all TWIM CCSs (Tables S4−S17).

RESULTS AND DISCUSSION

CCS Calibrants. The primary factors taken into consideration for choosing CCS calibrants to evaluate for use with phospholipids were: (i) ability to ionize in both positive and negative modes and/or (ii) structural similarity to phospholipids. Figure 1a summarizes the four types of calibrants evaluated: polyalanine (PolyAla, $n = 12(+)/14(−)$),[41] tetralkylammonium (TAA, $n = 8$) salts,[26,45] hexakis-(fluoroalkoxy)phosphazines (HFAP, $n = 4$), and glycerophospholipids (PC, $n = 10$; PE, $n = 14$) (see Figure S1 for the CCS plot in negative mode). All the CCS values of the calibrants were measured on the same DTIM platform to achieve a fair comparison between the different calibrants (see Experimental Section). Collectively, the calibrants cover a range of *m/z* and CCS from approximately 200−1250 *m/z* and 125−350 Å^2, respectively, in both positive and negative modes (Figures 1b and S1; see Tables S1−S3 for DTIM CCS values). The PC, PolyAla, and HFAP calibrants were evaluated in both positive and negative ionization modes, whereas the TAA salts were analyzed in positive mode only, as TAA does not readily generate an anion form. Although larger analytes ($m/z \geq 2000$) are present in the HFAP mix, only the four ions covering the range *m/z* 300−1250 (+ESI) were used for CCS calibration purposes. Notably, the nonlipid calibrants exhibit both larger and smaller CCS values than those of the lipids within the same mass range. The conformational distribution of the calibrants in the CCS vs *m/z* 2D plot (Figure 1 and Figure S1) suggests that the molecular packing efficiencies, or gas-phase densities, of these ions in the gas phase increase in the order of TAA ≪ PC ≈ PE < PolyAla ≪ HFAP in the positive mode and PC < PE < PolyAla ≪ HFAP in the negative mode. These trends can be reasonably understood based on their structures: each TAA contains four flexible hydrocarbon chains; each phospholipid contains two flexible fatty ester chains; each PolyAla is comprised of the same monomer (i.e., alanine) and can potentially form compact structures via intramolecular hydrogen bonding; and each HFAP is made of a rigid aromatic ring and heavier atoms such as fluorine and phosphorus that greatly increase the density of the structure relative to other calibrants of similar *m/z*.
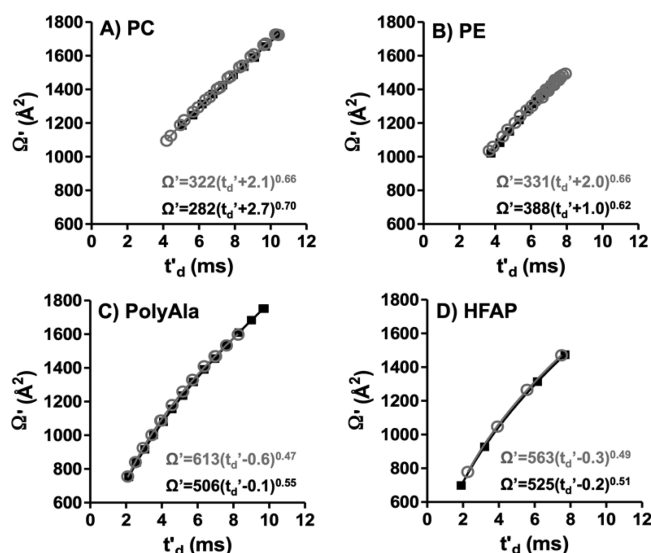
Figure 2. TWIM CCS calibration plots for A) PC, B) PE, C) PolyAla, and (D) HFAP CCS calibrants, where Ω' is the corrected drift tube CCS and t_d' is the mass-independent drift time. Calibration was performed with wave settings of 40 V and 550 m/s. Plots from positive (open gray circles) and negative (filled black squares) mode analyses are overlaid. The calibration equations for each mode are also shown. All calibration fits had $R^2 \geq 0.995$.

In positive mode, the majority of the CCS calibrants demonstrate strong power relationships between CCS and m/z, with $R^2 > 0.99$ for TAA, PolyAla, PCs (+ H and + Na), and HFAPs when fit to the equation $y = ax^b$.[26] The TAA salts display the largest exponent value being 0.625, followed by PCs (0.575), PEs (0.529), PolyAla (0.496), and HFAPs (0.451). The PEs had the poorest fit ($R^2 = 0.988$) due to the number of PEs with one or two unsaturated fatty acids ($n = 5$) versus those with fully saturated fatty acids ($n = 9$). Excluding PEs with unsaturated fatty acids improved the fit of the PE mobility-mass correlation for both the protonated and sodium coordinated species ($R^2 = 0.9995$), while the unsaturated PEs alone have an $R^2 = 0.806$ (Figure S2). In negative mode, linear regression analysis provided a better fit to the data (all $R^2 > 0.99$) than the power fitting for all calibrants (HFAPs, PolyAla, PCs, PEs), suggesting that the relationship between CCS and m/z is more linear in negative mode.

Comparison of Different Calibrants on Lipid CCS Measurement. A principal goal of this work is to evaluate the cross-calibration of each class of phospholipids (i.e., PCs to calibrate PEs and PEs to calibrate PCs), in comparison with other classes of calibrants: PolyAla, HFAP, and TAA. For the TWIM analysis, we chose to carry out initial studies at a wave velocity of 550 m/s and wave height of 40 V since these conditions were observed to give maximum separation of the lipid ions without carrying over the ions to the next IM cycle. Figure 2 contains representative TWIM CCS calibration curves for PC, PE, PolyAla, and HFAP from both positive (open gray circles) and negative (filled black squares) mode analyses, which were obtained using eq 1. For all analytes investigated, the resulting calibration curves yielded regression values greater than 0.995 with averaged calibration fit errors from 0.1 to 0.5% (Tables S4−S9). The most notable difference between the calibration curves for the different calibrants is in the degree of curvature in the fit. For example, the calibration curves for PolyAla (Figure 2c) and HFAP (Figure 2d), as well as TAA

(Figure S3), are slightly curved. However, calibration curves for PE and PC are distinctly more linear as indicated by the values of exponent B in eq 1 being closer to one. Comparison of the fit parameter for the phospholipids relative to the other calibrants shows that PEs and PCs yielded smaller values for fit parameter A' and positive values greater than 1 for t_0, whereas the other calibrants had larger values of A' and negative values below 1 for t_0. These differences in fitting parameters provide further evidence that lipid-specific calibrants are needed in order to achieve the most accurate measurement of lipid CCS using TWIM.

The effects of using calibration curves such as those for PolyAla, TAA, HFAP, and the phospholipids to calculate CCS values for PEs and PCs can be seen in Figure 3 (detailed calibration errors in Tables S10−S17), which presents the calibrated CCSs and the ±2% CCS bands (black dashed lines) based on the DTIM CCSs. For positive mode analysis of PCs (Figure 3a), calibration with PolyAla and TAAs yield some cross sections that deviate significantly ($\geq 2\%$) from CCS values measured on the DTIM instrumentation, notably within the intermediate mass range. A similar trend is observed for PCs in negative mode (Figure 3b), where PolyAla yields calibrated CCSs that have errors greater than +2% CCS for intermediate masses. Calibration of PCs with HFAP and PEs provided the most accurate results with errors within ±2% CCS in both positive and negative modes.

For positive mode analysis of PEs (Figure 3c), PolyAla and TAA calibrated CCS values increasingly deviate from the DTIM CCSs as the PE species increase in mass and size. The PolyAla calibration errors are predominantly within the +2% CCS band, but calibration errors for TAA-calibrated PEs exceed +2% starting with PE 10:0/10:0 at m/z 524.3. Alternatively, calibration of PEs with HFAP yields CCSs with negative error in the low mass region and positive error in the high mass region. The use of PCs for CCS calibration of PEs works well in positive mode, with all calibrated CCSs within ±2% of the DTIM CCSs. Calibration of PEs with PolyAla in negative mode (Figure 3d) has a trend similar to that observed in positive mode; however, the errors are greater than 2% CCS for all PE species. As with the calibrated PC results, the HFAP-calibrated PE CCS values in negative mode are well within 2% error from the DTIM values. Calibration of PEs with PCs in negative mode also yielded favorable results, with only PE 6:0/6:0 and 8:0/8:0 displaying errors great than 2%.

Overall, at wave velocity of 550 m/s and wave height of 40 V, PCs and PEs performed the best as the lipid CCS calibrants (see Table S4 for a summary of precision and accuracy of the calibrants). In positive mode, average calibration errors comparable to the fit errors (i.e., 0.1−0.5% error) observed from the PC and PE calibration curves themselves. Average errors were higher in negative mode but remained below 1% error. Calibration with HFAP also provided accurate CCSs for PEs and PCs in both ionization modes, with average errors $\leq 1\%$.

Effect of Wave Velocity and Wave Height on Lipid CCS Calibration. To evaluate the performance of PEs, PCs, and HFAP as lipid CCS calibrants under different traveling wave parameters, the above experiments were repeated using varied combinations of wave height (40, 35, and 30 V) and wave velocity (550, 500, and 450 m/s). Calibration of PEs and PCs with HFAP yielded the largest average percent errors in positive mode (Tables S18 and S20) due to dependencies on both mass and traveling wave parameters. The error of the CCS
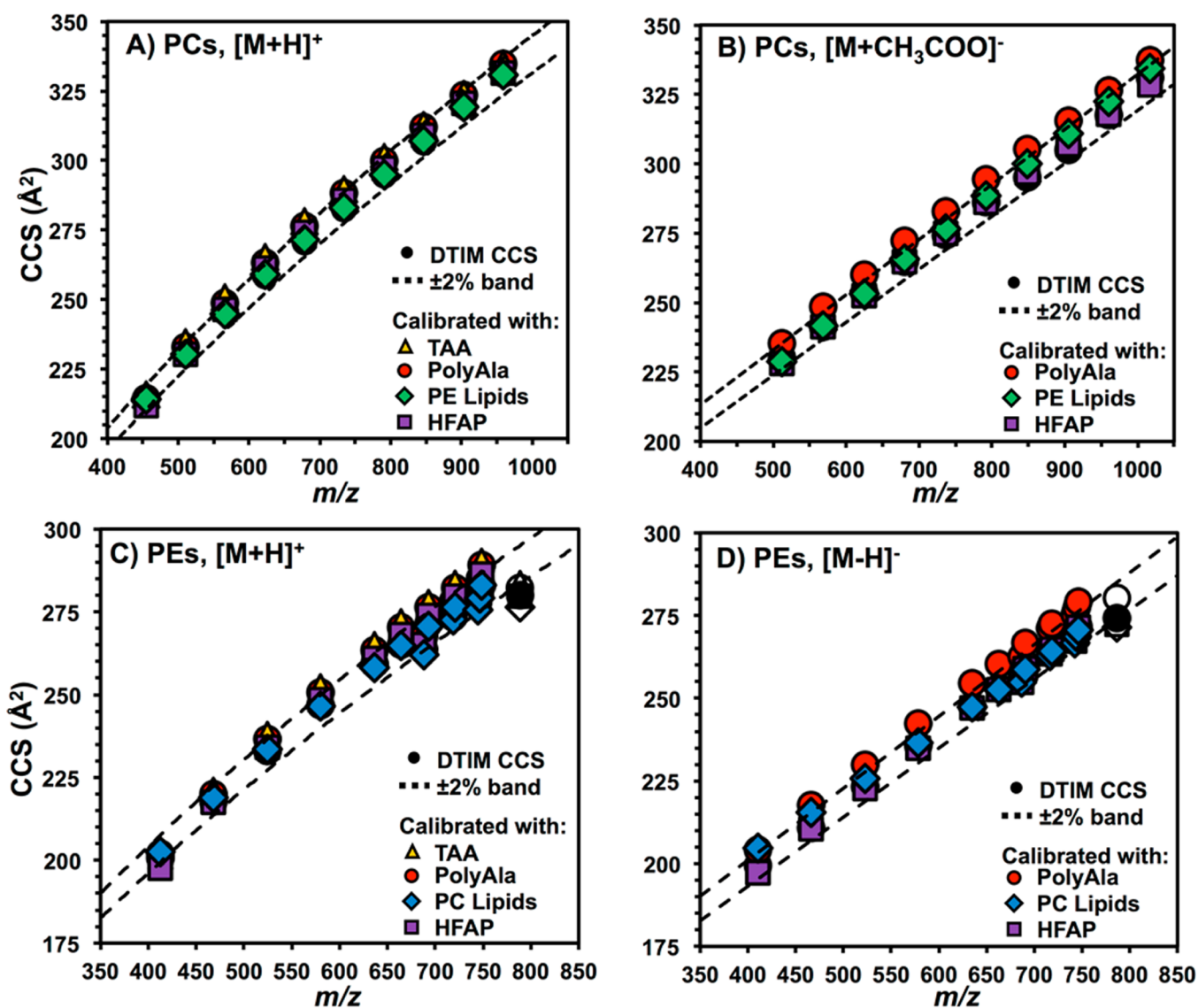
Figure 3. Comparison of the accuracies of TWIM CCS calibrants for PCs (A and B) and PEs (C and D) at 550 m/s and 40 V. Each symbol represents averaged ($n = 9$) calibrated CCS values from a different calibrant. The dashed lines represent ±2% error from the drift tube (DT) CCS values (black circles), fit to power functions in parts A and C and linear functions in parts B and D. Calibrated CCSs for PE 20:4/20:4 are shown as open markers in parts C and D as the DTIM CCS of PE 20:4/20:4 was excluded from the fit of the ±2% error lines. For clarity, only protonated adducts are shown in parts A and C.

calibration decreased with decreasing wave height for both PEs and PCs (Figures S4 and S6), while calibration error increased with decreasing wave velocity (i.e., lowest errors at 550 m/s and 30 V). The effects of traveling wave parameters on calibration error were small in negative mode, where errors across all species and combinations of wave height and velocity were within ±2% CCS. For HFAP-calibration of PEs, the errors were relatively consistent over the mass range with the exception of PE 20:4/20:4, which showed greater average calibration errors in positive and negative modes. HFAP-calibrated PC species, on the other hand, exhibited larger errors in the middle of the calibration range which was most pronounced in positive mode, where the absolute error ranged from −0.5% for PC 6:0/6:0 to +2.5% for the intermediate PC species (i.e., PC 14:0/14:0−18:0/18:0).

Trends were also observed in positive and negative modes for CCS calibration with phospholipids at varied wave heights and wave velocities. Calibration of PCs with PEs showed clear

bias toward smaller PCs in positive mode, with consistently small calibration errors up to PC 18:0/18:0 (<0.5%), and larger errors for PC 20:0/20:0 to 24:0/24:0 (−0.5% to −2.5%) (Figure 4A and Figure S7). The reverse effect was observed for CCS calibration of PEs with PCs in negative mode, where calibration errors were +0.5% to +3.5% for PEs 6:0/6:0 to 12:0/12:0 over all combinations of wave height and velocity (Figure 4D and Figure S5). Calibration errors for PC-calibrated PE CCSs in positive mode and PE-calibrated PC CCSs in negative mode were consistently low across all TWIM parameters with only PC 24:0/24:0 displaying errors greater than 1% (Figure 4B,C and Figures S5 and S7). In general, the calibration bias appears to become more evident as the wave velocity decreases, i.e., CCSs with large calibration errors tend to display even larger errors at smaller wave velocity while the CCSs with smaller errors are relatively consistent at all wave height and velocity (Figure 4 and Figures S5 and S7). These observations may be due to the fact that in TWIM, under the
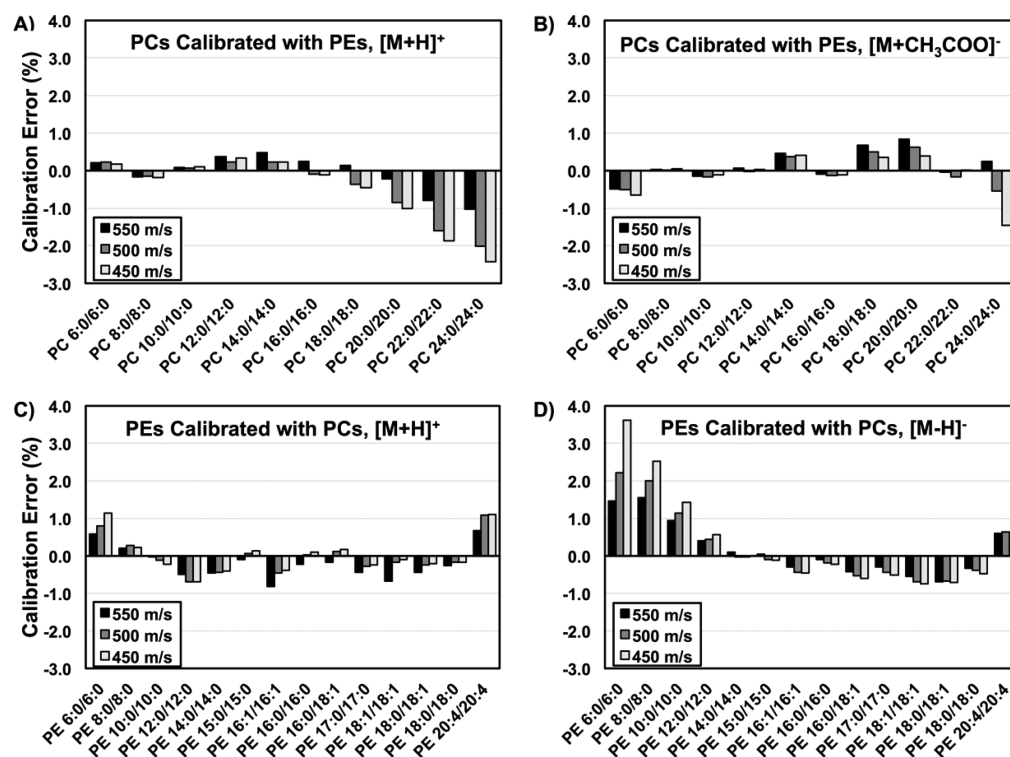
Figure 4. Effects of traveling wave velocity on CCS calibration accuracy: (A) calibration of protonated PCs with PE CCSs in positive mode, (B) calibration of PCs with PE CCS in negative mode, (C) calibration of protonated PEs with PC CCSs in positive mode, (D) calibration of PEs with PC CCSs in negative mode. A traveling wave height of 40 V was used for all measurements.

conditions of lower wave heights and higher wave velocities, the ions experience more structurally selective roll-over events which better describe differences in their gas-phase structure,[36] and the corresponding longer drift times would also serve to reduce the magnitude of time measurement errors, such as bin averaging and IM peak centroiding.

Overall, PCs and PEs outperformed HFAP as the calibrants for lipids even though all three CCS calibrants displayed some calibration errors that were dependent upon mass, size, or traveling wave parameters. Additional experiments performed with a ramped wave velocity also demonstrate the inconsistency of HFAP as CCS calibrants. Using a linearly ramped wave velocity range of 900−300 m/s and a fixed wave height of 40 V, the performance of PE and PC calibrants was consistent with results obtained under static wave velocities whereas the performance of HFAP diminished greatly when using the ramped wave velocity (Tables S22−S25). The inconsistencies in the performance of HFAP as generalized CCS calibrants for TWIM is likely the result of the low number of HFAP species (n = 4) used in these experiments. Although the HFAP ions chosen adequately bracket the mass range typically observed for lipids, the limited number of HFAP calibrants within the lipid m/z range was not sufficient to provide robust and accurate calibration of lipid CCSs.

While the use of phospholipids as TWIM CCS calibrants yielded the most accurate calibrated CCSs for both PEs and PCs, the mass-dependent calibration errors observed for PE-calibrated PC CCSs in positive mode and PC-calibrated PE CCSs in negative mode merit further discussion (Figure 4A,D). For PC-calibrated PE CCSs in negative mode, the increase in calibration errors with decreasing PE mass can likely be attributed to the different negative ion species formed between PEs and PC lipids, specifically deprotonated and acetate-

adducted, respectively. While the PC headgroup is 44 Da larger than the PE headgroup for the neutral species, this mass difference becomes even larger when analyzing the negative ions due to the need to form adducts for negative mode ionization of PC species. The formation of acetate adducts (+ 59 Da) was chosen for this analysis due to the frequent use of ammonium acetate as a buffer in LC solvents, particularly for reverse phase and HILIC methods. However, the formation of acetate adducts led to larger proportion of structural changes to the PCs with shorter acyl chains (10:0/10:0 or smaller) than those with longer acyl chains. As a result, acetate adduction decreases the structural similarity of PC negative ions relative to PE negative ions with similar fatty acid compositions. It has been reported that different metal ion adducts of PCs significantly affect their CCS mobility-mass correlations in the positive mode, with the bigger metal ions displaying a larger effect.[21] On the other hand, the increased calibration errors observed in positive mode for PE-calibrated PC CCSs with acyl chains of 20 carbons or greater likely results from the lack of PE calibrant species above 800 Da.

Unsaturation in the acyl chains was found to affect the CCS and the calibration accuracy. CCS measurements of PEs possessing the same number of carbons and increasing degrees of unsaturation (i.e., PE 18:0/18:0, 18:0/18:1, and 18:1/18:1 in Table S1) demonstrate that the addition of double bonds leads to a reduction in the CCS. Kim et al. have reported similar observations for the addition of double bonds to the acyl chains of PCs, where the first double bond led to a 5% reduction in drift time with a further 1% reduction for each additional double bond.[39] The reduction in CCS observed for additional double bonds in PEs was 0.3 and 0.9% for acyl chains lengths of 18 and 16, respectively, but no bias was observed in the CCS calibration of saturated versus singly- or doubly unsaturated

PEs. The single highly unsaturated PE evaluated in this study, PE 20:4, deviated significantly (approximately 6%) from the PE and PC trendline in the CCS vs. m/z plot (Figure 1b) and tended to have greater calibration errors than PEs with fewer or no double bonds (Tables S5 and S11), although all errors were within ±2% when calibration was performed with PCs. Thus, a set of highly unsaturated phospholipid CCS calibrants may be of benefit if TWIM CCS information for highly unsaturated phospholipids is desired.

Validation of the Performance of Lipid CCS Calibrants. To evaluate the performance of the lipid CCS calibrants in an untargeted lipidomics experiment, TWIM CCSs were obtained for the components in SM, PS, PE, and PC extracts and compared against their DTIM CCS values.[26,52] The results from triplicate measurements of the most abundant SMs and PSs (n = 5 each) are shown in Table 1 (additional

Table 1. Validation of Lipid CCS Calibration against DTIM Measurements of SM and PS Extracts

identification[a]	m/z observed	TWIM CCS (Å²) [adduct]	DTIM CCS (Å²) [adduct]	CCS error (%)	RSD (%) TWIM CCS
SM 34:01	703.58	278.7 [H]	280.1 [H]	−0.5	0.2
SM 36:01	731.61	284.7 [H]	286.2 [H]	−0.5	0.1
SM 40:02	785.65	297.6 [H]	295.7 [H]	0.6	0.1
SM 42:02	813.69	304.0 [H]	301.4 [H]	0.9	0.0
SM 42:01	815.70	305.2 [H]	303.2 [H]	0.6	0.0
PS 38:04	812.54	281.3 [H]	284.4 [H]	−1.1	0.2
PS 38:02	816.58	282.6 [H]	287.7 [H]	−1.8	0.4
PS 38:01	818.59	283.3 [H]	289.6 [H]	−2.2	0.5
PS 40:06	836.55	284.3 [H]	287.7 [H]	−1.2	0.2
PS 40:05	838.56	286.1 [H]	289.6 [H]	−1.2	0.2

[a]All identifications made within 10 ppm of the observed m/z.

results in Table S26). Notably, the absolute errors between DTIM and TWIM CCSs were below 2% with the exception of only two lipid species (PS 38:01 and PC 36:1) at 2.2%. The outstanding performance of these lipid calibrants on lipid classes other than PE and PC suggest that these calibrants may have broad application in measurement of CCS of polar lipids using TWIM.

CONCLUSIONS

While several sets of calibrants have been proposed for generating calibrated CCSs from TWIM-MS platforms, we have found that the use of structurally matched calibrants provides greater accuracy of calibrated CCS for phospholipids than PolyAla and TAAs and greater consistency over multiple traveling wave parameters than HFAPs. On the basis of the observations described above, the best implementation of the proposed phospholipid CCS calibrants was determined to be the use of PCs for CCS calibration of phospholipids in positive mode and the use of PEs for CCS calibration of phospholipids in negative mode. We believe this work will equally benefit those laboratories who may choose to use PolyAla for its ease-of-use and cost-effectiveness, in that the inherent errors of using PolyAla to calibrate lipid CCSs are demonstrated here for the first time. Although the cost of purchasing individual standards is greater than that of premixed calibrants, the expense is justifiable given the improved accuracy of calibrated CCSs provided by the lipid calibrants relative to PolyAla or HFAP. The development of phospholipid CCS calibrants will enable

high-accuracy structural studies of lipids and add an additional level of validation in the assignment of identifications in untargeted lipidomics experiments.

ASSOCIATED CONTENT

Ⓢ Supporting Information

. The Supporting Information is available free of charge on the ACS Publications website at DOI: 10.1021/acs.analchem.6b01728.

Drift tube CCS measurements for calibrant species; summary of CCS calibration accuracies and precisions; detailed results for each PE and PC species from interday CCS calibration analysis, including relative standard deviations (RSD, %) of interday measurements of calibrated CCS accuracy (% error); graphical and tabular depictions of the effect of traveling wave height and velocity of CCS calibration accuracy; summarized results for the performance of CCS calibrants with ramped wave velocities; and comparison of calibrated and drift tube CCS measurement of PEs and PCs in lipid extracts (PDF)

AUTHOR INFORMATION

Corresponding Author
*Phone: (206) 543-1080. Fax: (206) 685-3252. E-mail: libinxu@uw.edu.

Notes
The authors declare no competing financial interest.

REFERENCES

(1) Yeagle, P. L. *FASEB J.* **1989**, *3*, 1833.
(2) Wymann, M. P.; Schneiter, R. *Nat. Rev. Mol. Cell Biol.* **2008**, *9*, 162.
(3) Berliner, J. A.; Leitinger, N.; Tsimikas, S. *J. Lipid Res.* **2008**, *50*, S207.
(4) Santos, C. R.; Schulze, A. *FEBS J.* **2012**, *279*, 2610.
(5) Sounni, N. E.; Cimino, J.; Blacher, S.; Primac, I.; Truong, A.; Mazzucchelli, G.; Paye, A.; Calligaris, D.; Debois, D.; De Tullio, P.; Mari, B.; De Pauw, E.; Noel, A. *Cell Metab.* **2014**, *20*, 280.
(6) Gross, R. W.; Han, X. *Methods Enzymol.* **2007**, *433*, 73.
(7) Schmelzer, K.; Fahy, E.; Subramaniam, S.; Dennis, E. A. *Methods Enzymol.* **2007**, *432*, 171.
(8) Quehenberger, O.; et al. *J. Lipid Res.* **2010**, *51*, 3299.
(9) Dennis, E. A.; Deems, R. A.; Harkewicz, R.; Quehenberger, O.; Brown, H. A.; Milne, S. B.; Myers, D. S.; Glass, C. K.; Hardiman, G.; Reichart, D.; Merrill, A. H., Jr.; Sullards, M. C.; Wang, E.; Murphy, R.

C.; Raetz, C. R.; Garrett, T. A.; Guan, Z.; Ryan, A. C.; Russell, D. W.; McDonald, J. G.; Thompson, B. M.; Shaw, W. A.; Sud, M.; Zhao, Y.; Gupta, S.; Maurya, M. R.; Fahy, E.; Subramaniam, S. *J. Biol. Chem.* **2010**, *285*, 39976.

(10) Quehenberger, O.; Dennis, E. A. *N. Engl. J. Med.* **2011**, *365*, 1812.

(11) Han, X.; Gross, R. W. *Mass Spectrom. Rev.* **2005**, *24*, 367.

(12) Schwudke, D.; Liebisch, G.; Herzog, R.; Schmitz, G.; Shevchenko, A. *Methods Enzymol.* **2007**, *433*, 175.

(13) Merrill, A. H., Jr.; Sullards, M. C.; Allegood, J. C.; Kelly, S.; Wang, E. *Methods* **2005**, *36*, 207.

(14) Ivanova, P. T.; Milne, S. B.; Byrne, M. O.; Xiang, Y.; Brown, H. A. *Methods Enzymol.* **2007**, *432*, 21.

(15) Clemmer, D. E.; Hudgins, R. R.; Jarrold, M. F. *J. Am. Chem. Soc.* **1995**, *117*, 10141.

(16) von Helden, G.; Wyttenbach, T.; Bowers, M. T. *Science* **1995**, *267*, 1483.

(17) McLean, J. A.; Ruotolo, B. T.; Gillig, K. J.; Russell, D. H. *Int. J. Mass Spectrom.* **2005**, *240*, 301.

(18) Kanu, A. B.; Dwivedi, P.; Tam, M.; Matz, L.; Hill, H. H., Jr. *J. Mass Spectrom.* **2008**, *43*, 1.

(19) May, J. C.; McLean, J. A. *Anal. Chem.* **2015**, *87*, 1422.

(20) Jackson, S. N.; Wang, H. Y.; Woods, A. S.; Ugarov, M.; Egan, T.; Schultz, J. A. *J. Am. Soc. Mass Spectrom.* **2005**, *16*, 133.

(21) Jackson, S. N.; Ugarov, M.; Post, J. D.; Egan, T.; Langlais, D.; Schultz, J. A.; Woods, A. S. *J. Am. Soc. Mass Spectrom.* **2008**, *19*, 1655.

(22) Fenn, L. S.; McLean, J. A. *Anal. Bioanal. Chem.* **2008**, *391*, 905.

(23) Fenn, L. S.; Kliman, M.; Mahsut, A.; Zhao, S. R.; McLean, J. A. *Anal. Bioanal. Chem.* **2009**, *394*, 235.

(24) Paglia, G.; Angel, P.; Williams, J. P.; Richardson, K.; Olivos, H. J.; Thompson, J. W.; Menikarachchi, L.; Lai, S.; Walsh, C.; Moseley, A.; Plumb, R. S.; Grant, D. F.; Palsson, B. O.; Langridge, J.; Geromanos, S.; Astarita, G. *Anal. Chem.* **2015**, *87*, 1137.

(25) Groessl, M.; Graf, S.; Knochenmuss, R. *Analyst* **2015**, *140*, 6904.

(26) May, J. C.; Goodwin, C. R.; Lareau, N. M.; Leaptrot, K. L.; Morris, C. B.; Kurulugama, R. T.; Mordehai, A.; Klein, C.; Barry, W.; Darland, E.; Overney, G.; Imatani, K.; Stafford, G. C.; Fjeldsted, J. C.; McLean, J. A. *Anal. Chem.* **2014**, *86*, 2107.

(27) Kliman, M.; May, J. C.; McLean, J. A. *Biochim. Biophys. Acta, Mol. Cell Biol. Lipids* **2011**, *1811*, 935.

(28) Giles, K.; Pringle, S. D.; Worthington, K. R.; Little, D.; Wildgoose, J. L.; Bateman, R. H. *Rapid Commun. Mass Spectrom.* **2004**, *18*, 2401.

(29) Pringle, S. D.; Giles, K.; Wildgoose, J. L.; Williams, J. P.; Slade, S. E.; Thalassinos, K.; Bateman, R. H.; Bowers, M. T.; Scrivens, J. H. *Int. J. Mass Spectrom.* **2007**, *261*, 1.

(30) Ridenour, W. B.; Kliman, M.; McLean, J. A.; Caprioli, R. M. *Anal. Chem.* **2010**, *82*, 1881.

(31) Kyle, J. E.; Zhang, X.; Weitz, K. K.; Monroe, M. E.; Ibrahim, Y. M.; Moore, R. J.; Cha, J.; Sun, X.; Lovelace, E. S.; Wagoner, J.; Polyak, S. J.; Metz, T. O.; Dey, S. K.; Smith, R. D.; Burnum-Johnson, K. E.; Baker, E. S. *Analyst* **2016**, *141*, 1649.

(32) Mason, E. A.; Schamp, H. W., Jr *Ann. Phys.* **1958**, *4*, 233.

(33) Mason, E. A.; McDaniel, E. W. *Transport Properties of Ions in Gases*; Wiley: New York, 1988.

(34) Shvartsburg, A. A.; Smith, R. D. *Anal. Chem.* **2008**, *80*, 9689.

(35) Giles, K.; Wildgoose, J. L.; Langridge, D. J.; Campuzano, I. *Int. J. Mass Spectrom.* **2010**, *298*, 10.

(36) May, J. C.; McLean, J. A. *Int. J. Ion Mobility Spectrom.* **2013**, *16*, 85.

(37) Scarff, C. A.; Thalassinos, K.; Hilton, G. R.; Scrivens, J. H. *Rapid Commun. Mass Spectrom.* **2008**, *22*, 3297.

(38) Ruotolo, B. T.; Benesch, J. L.; Sandercock, A. M.; Hyung, S. J.; Robinson, C. V. *Nat. Protoc.* **2008**, *3*, 1139.

(39) Kim, H. I.; Kim, H.; Pang, E. S.; Ryu, E. K.; Beegle, L. W.; Loo, J. A.; Goddard, W. A.; Kanik, I. *Anal. Chem.* **2009**, *81*, 8289.

(40) Smith, D. P.; Knapman, T. W.; Campuzano, I.; Malham, R. W.; Berryman, J. T.; Radford, S. E.; Ashcroft, A. E. *Eur. Mass Spectrom.* **2009**, *15*, 113.

(41) Bush, M. F.; Campuzano, I. D.; Robinson, C. V. *Anal. Chem.* **2012**, *84*, 7124.

(42) Forsythe, J. G.; Petrov, A. S.; Walker, C. A.; Allen, S. J.; Pellissier, J. S.; Bush, M. F.; Hud, N. V.; Fernandez, F. M. *Analyst* **2015**, *140*, 6853.

(43) Thalassinos, K.; Grabenauer, M.; Slade, S. E.; Hilton, G. R.; Bowers, M. T.; Scrivens, J. H. *Anal. Chem.* **2009**, *81*, 248.

(44) Bush, M. F.; Hall, Z.; Giles, K.; Hoyes, J.; Robinson, C. V.; Ruotolo, B. T. *Anal. Chem.* **2010**, *82*, 9557.

(45) Campuzano, I.; Bush, M. F.; Robinson, C. V.; Beaumont, C.; Richardson, K.; Kim, H.; Kim, H. I. *Anal. Chem.* **2012**, *84*, 1026.

(46) Paglia, G.; Williams, J. P.; Menikarachchi, L.; Thompson, J. W.; Tyldesley-Worster, R.; Halldorsson, S.; Rolfsson, O.; Moseley, A.; Grant, D.; Langridge, J.; Palsson, B. O.; Astarita, G. *Anal. Chem.* **2014**, *86*, 3985.

(47) Zhang, L.; Vertes, A. *Anal. Chem.* **2015**, *87*, 10397.

(48) Beegle, L. W.; Kanik, I.; Matz, L.; Hill, H. H. *Int. J. Mass Spectrom.* **2002**, *216*, 257.

(49) Matz, L. M.; Hill, H. H., Jr.; Beegle, L. W.; Kanik, I. *J. Am. Soc. Mass Spectrom.* **2002**, *13*, 300.

(50) Gelb, A. S.; Jarratt, R. E.; Huang, Y.; Dodds, E. D. *Anal. Chem.* **2014**, *86*, 11396.

(51) May, J. C.; Dodds, J. N.; Kurulugama, R. T.; Stafford, G. C.; Fjeldsted, J. C.; McLean, J. A. *Analyst* **2015**, *140*, 6824.

(52) Leaptrot, K. L.; May, J. C.; Dodds, J. N.; McLean, J. A. 2016, in preparation.